No. SOC-194

OPTIMIZATION AND DESIGN CENTERING OF ACTIVE AND NONLINEAR CIRCUITS INCLUDING COMPONENT TOLERANCES AND MODEL UNCERTAINTIES

J.W. Bandler, H.L. Abdel-Malek,
P. Dalsgaard, Z.S. El-Razaz and M.R.M. Rizk

April 1978

OPTIMIZATION AND DESIGN CENTERING OF ACTIVE AND NONLINEAR CIRCUITS INCLUDING COMPONENT TOLERANCES AND MODEL UNCERTAINTIES

J.W. Bandler, H.L. Abdel-Malek, P. Dalsgaard,

Z.S. El-Razaz and M.R.M. Rizk

Abstract

Significant new results permit exploitation of general and special-purpose simulators to optimally center, tolerance and tune circuits including statistics, parasitics and model uncertainties. A nonlinear switching circuit and a tunable active filter demonstrate the procedure. The filter has been optimized in a variety of ways taking into account nonideal operational amplifiers employing both SPICE2 and a specially written analysis program. The switching circuit has been treated via the state equations, the companion network approach with results confirmed separately by SPICE2.

This work was supported by the National Research Council of Canada under grant A7239 and by the Danish Council for Scientific and Industrial Research through support to P. Dalsgaard.

J.W. Bandler, H.L. Abdel-Malek, Z.S. El-Razaz and M.R.M. Rizk are with the Group on Simulation, Optimization and Control and Department of Electrical Engineering, McMaster University, Hamilton, Canada L8S 4L7.

P. Dalsgaard is with the Institute of Electronic Systems, Aalborg University, Aalborg, Denmark.

II. THE TOLERANCE PROBLEM

Associated with the k-element vector of design variables, denoted $\underset{\sim}{\phi}$, we have the nominal parameter vector $\underset{\sim}{\phi}^0$ and the vector of manufacturing tolerances $\underset{\sim}{\varepsilon}$. Furthermore [1, 6], we may also consider $\underset{\sim}{t}_m$ and $\underset{\sim}{t}_c$ distinguishing, respectively, the tuning available to the manufacturer (for improving the performance) and to the customer (to meet a variety of desired specifications).

Thus, $\underset{\sim}{\phi}$ will indicate, in general, actual values of the design parameters following tolerance and tuning effects. The ith component is given by

$$\phi_i = \phi_i^0 + \varepsilon_i \mu_{\varepsilon i} + t_{mi} \mu_{tmi} + t_{ci} \mu_{tci} \ , \tag{1}$$

where we also note, explicitly, the ith components of $\underset{\sim}{\mu}_\varepsilon$, $\underset{\sim}{\mu}_{tm}$ and $\underset{\sim}{\mu}_{tc}$.

The k-vector $\underset{\sim}{\mu}_\varepsilon$ (uncontrollable) determines a particular design outcome, whereas the vectors $\underset{\sim}{\mu}_{tm}$ and $\underset{\sim}{\mu}_{tc}$ (controllable) determine, respectively, settings of tuning variables by manufacturer and customer.

Intuitively, $\underset{\sim}{\mu}_\varepsilon$, $\underset{\sim}{\mu}_{tm}$ and $\underset{\sim}{\mu}_{tc}$ represent deviations or adjustments of a given design, while $\underset{\sim}{\phi}^0$, $\underset{\sim}{\varepsilon}$, $\underset{\sim}{t}_m$ and $\underset{\sim}{t}_c$ characterize a given production set-up.

Fig. 1 illustrates a set of frequency domain specifications to be met by tuning an available parameter. Fig. 2 depicts the corresponding situation in the parameter space. One toleranced variable, one tunable variable set by the manufacturer and one customer tunable variable are represented. Three settings of the tunable variable corresponding to the three settings in Fig. 1 are shown.

In parallel with the foregoing discussion we can introduce the n-element model parameter vector $\underset{\sim}{p}$, the corresponding vector of nominal values $\underset{\sim}{p}^0$ and the vector of model uncertainties $\underset{\sim}{\mu}_\delta$.

Use of SPICE2

The program SPICE2 [5] has been used to obtain circuit responses at the base points needed for the modeling. The program can be run with different sets of parameter values. In order to reduce the overhead time, and assuming that the circuit is not very large, the program can be used only once by supplying the data in such a way that the circuit is repeated with different sets of nodes (where there is no interconnection between each set of nodes except the ground node) with different sets of parameter values. In the frequency domain case the overall nodal admittance matrix is, consequently, block diagonal matrix with each block representing a $\underset{\sim}{Y}$ matrix of the circuit. Fig. 4 shows such an example.

IV. THE TUNABLE ACTIVE FILTER

We consider here the design of a tunable active filter (Fig. 5) to meet design specifications in the worst-case sense everywhere in the range of the tunable parameter. The active filter is based on an active bandpass realization considered by Budak and Zeller [8]. It is a variable center frequency design, nominally constant bandwidth and constant peak value. The center frequency is variable by considering one element, namely, R_4. The operational amplifier(s) employed are taken as nonideal, in particular, the one-pole roll-off model given by

$$A(s) = \frac{A_0 \omega_a}{s+\omega_a} , \tag{4}$$

$$\begin{bmatrix} G_1+G_g & 0 & -G_1 & 0 \\ 0 & G_2+G_3+sC_2+A_2G_3 & -sC_2 & -G_2+A_1A_2G_3 \\ -G_1 & -sC_2 & G_1+G_4+sC_1+sC_2 & -sC_1 \\ 0 & -G_2 & -sC_1 & G_2+sC_1 \end{bmatrix} \begin{bmatrix} V_1 \\ V_2 \\ V_3 \\ V_4 \end{bmatrix} = \begin{bmatrix} G_gV_g \\ 0 \\ 0 \\ 0 \end{bmatrix} , \quad (9)$$

where $G_3 = 1/R$.

The specifications w.r.t. frequency f are

$F \leq 1/\sqrt{2}$ for $f \leq f_0 - 10$ Hz,

$F \leq 1.1$ for $f_0 - 10 \leq f \leq f_0 + 10$ Hz,

$F \leq 1/\sqrt{2}$ for $f \geq f_0 + 10$ Hz,

$F \geq 1/\sqrt{2}$ for $f_0 - 8 \leq f \leq f_0 + 8$ Hz,

$F \geq 1$ for $f = f_0$ Hz,

where f_0 is the center frequency. Fixed or tunable problems have been solved with

$$100 \leq f_0 \leq 700 \text{ Hz} .$$

For the tunable problems we may identify

$$f_0 \equiv \psi .$$

Several approaches have been deployed. First consider the optimal assignment of tolerances ε_1 to R_1 and ε_2 to C_1 and C_2, where $C^0 = C_1^0 = C_2^0$ and R_1^0 are variables. Let $f_0 = 100$ Hz and consider R_4 a post-production tuning variable for each outcome. Fig. 7 shows the equivalent circuit for using SPICE2. Since the program does not handle A(s) of (4), the gain was represented by the transfer function of a small additional circuit. The ΔV term at the input to the second amplifier is modeled by a current leaving a node connecting two voltage controlled current sources which are controlled by the voltages to be subtracted.

All 8 vertices (tolerance extremes) were considered. An upper

Hz. The program TOLOPT [11] was used with an exact analysis program which provided sensitivities.

Four discrete bands were selected for values of f_0 equal to 100, 300, 500 and 700 Hz. Sensitivity considerations relating to extremes of $\hat{F}$ and Ω suggested the selection of vertices corresponding to $\underset{\sim}{\mu}^1 = [-1\ -1\ -1\ -1]^T$, $\underset{\sim}{\mu}^2 = [1\ -1\ -1\ -1]^T$ and $\underset{\sim}{\mu}^{13} = [-1\ -1\ 1\ 1]^T$ for the lower two bands and $\underset{\sim}{\mu}^4 = [1\ 1\ -1\ -1]^T$, $\underset{\sim}{\mu}^{15} = [-1\ 1\ 1\ 1]^T$ and $\underset{\sim}{\mu}^{16} = [1\ 1\ 1\ 1]^T$ for the upper two bands. An upper specification of 1.1 was taken at normalized frequencies of 1, $1 \pm 0.5/f_0$, $1 \pm 1/f_0$, $1 \pm 1.5/f_0$ and $1/\sqrt{2}$ at $1 \pm 10/f_0$. A lower specification of $1/\sqrt{2}$ was taken at $1 \pm 8/f_0$ and 1 at a normalized frequency of 1. The objective function was

$$U = \frac{R_1^0}{\epsilon_{R1}} + \frac{C^0}{\epsilon_{C2}} + \frac{C^0}{\epsilon_{C1}} + \frac{R_2^0}{\epsilon_{R2}} \quad . \tag{11}$$

Including 12 variables for R_4 the total number of variables was 19. TOLOPT carried out the optimization.

Table II summarizes the results obtained and Fig. 9 the responses for the active vertices.

V. THE CURRENT SWITCH EMITTER FOLLOWER

Consider the CSEF circuit shown in Fig. 10. This circuit was previously employed by Ho [12] for time-domain sensitivity calculations. For analysis purposes, we consider the decoupled equivalent circuit of the lossless transmission line shown in Fig. 11(a). Fig. 11(b) shows the charge control model to be used for each transistor. The charge control diode model corresponds to that of the emitter-base junction.

Table III lists the original values of the circuit parameters and model parameters. The original transmission line parameters are 50 Ω

approach. The resulting response is substantially similar to those in Fig. 12. The running time, however, was cut by an order of magnitude to 7 s.

Realistic statistical transistor models based on work of Balaban and Golembeski [20], e.g., a triangular distribution of current gain β with a peak at 60 and $40 \leq \beta \leq 100$ with consequent parameter correlations, were used. Yield optimization increased the yield from 39% to 89% in 1.9 CPU minutes (including modeling) for certain design constraints employing only 45 integrations for this 8-dimensional problem. The resulting nominal responses are shown in Fig. 14. Further details of this problem are available from Abdel-Malek [15] and Abdel-Malek and Bandler [21].

VI. CONCLUSIONS

Design centering, tolerance assignment, postproduction tuning, worst-case design and yield optimization have been applied in a realistic way to practical problems. The possible exploitation of general purpose simulators has been stressed, hence it is quite feasible to use available programs to carry out sophisticated optimal design at reasonable cost.

VII. REFERENCES

[1] J.W. Bandler, P.C. Liu and H. Tromp, "A nonlinear programming approach to optimal design centering, tolerancing and tuning", IEEE Trans. Circuits and Systems, vol. CAS-23, 1976, pp. 155-165.

[2] J.W. Bandler, P.C. Liu and H. Tromp, "Integrated approach to microwave design", IEEE Trans. Microwave Theory Tech., vol. MTT-24, 1976, pp. 584-591.

case design and yield optimization", Faculty of Engineering, McMaster University, Hamilton, Canada, Report SOC-182, 1977.

[16] H.L. Abdel-Malek and J.W. Bandler, "State equation analysis and computer program for a current switch emitter follower", Faculty of Engineering, McMaster University, Hamilton, Canada, Report SOC-192, 1978.

[17] H.L. Abdel-Malek and J.W. Bandler, "Subroutines for implementing quadratic models of surfaces in optimal design", Faculty of Engineering, McMaster University, Hamilton, Canada, Report SOC-191, 1978.

[18] M.R.M. Rizk, "Analysis of a current switch emitter follower using the companion network approach", Faculty of Engineering, McMaster University, Hamilton, Canada, Report SOC-193, 1978.

[19] D.A. Calahan, Computer-Aided Network Design (Revised Edition). New York: McGraw Hill, 1972.

[20] P. Balaban and J.J. Golembeski, "Statistical analysis for practical circuit design", IEEE Trans. Circuits and Systems, vol. CAS-22, 1975, pp. 100-108.

[21] H.L. Abdel-Malek and J.W. Bandler, "Yield optimization for arbitrary statistical distributions, Parts I and II", Proc. IEEE Int. Symp. Circuits and Systems (New York, NY, 1978).

TABLE III(a)

CIRCUIT PARAMETER VALUES

R_1	281.33 Ω
R_2	75.00 Ω
R_3	78.24 Ω
R_4	50.00 Ω
E_2	4.03 V
E_3	1.13 V
E_4	1.70 V
C_0	1.50 pF

TABLE III(b)

DIODE MODEL PARAMETERS

I_{SD}	diode saturation current	0.6×10^{-9} A
C_{JD}	depletion layer capacitance	0.12 pF
TT_D	transit time	0.01 ns
θ	inverse of thermal potential	38.668 V^{-1}

$$I_D = I_{SD}(\exp(\theta V_D)-1)$$

$$C_D = C_{JD} + TT_D \frac{dI_D}{dV_D}$$

FIGURE CAPTIONS

Fig. 1 A set of frequency domain specifications for different settings of a tunable parameter.

Fig. 2 Parameter space representation of tolerance and tuning concepts.

Fig. 3 Arrangement of the base points w.r.t. the centers of interpolation regions in (a) two dimensions and (b) three dimensions.

Fig. 4 The circuit supplied to SPICE2 which is the original circuit repeated (k+1)(k+2)/2 times with appropriate parameter values.

Fig. 5 Tunable active filter with R_g = 50 Ω, R = 75 Ω and one-pole roll-off for A(s).

Fig. 6 Equivalent circuit for nodal analysis of the circuit of Fig. 5.

Fig. 7 Equivalent circuit for SPICE2 analysis of the circuit of Fig. 5.

Fig. 8 Fixed specifications: tuned optimal worst-case responses.

Fig. 9 Tunable specifications over 100-700 Hz: optimal worst-case response.

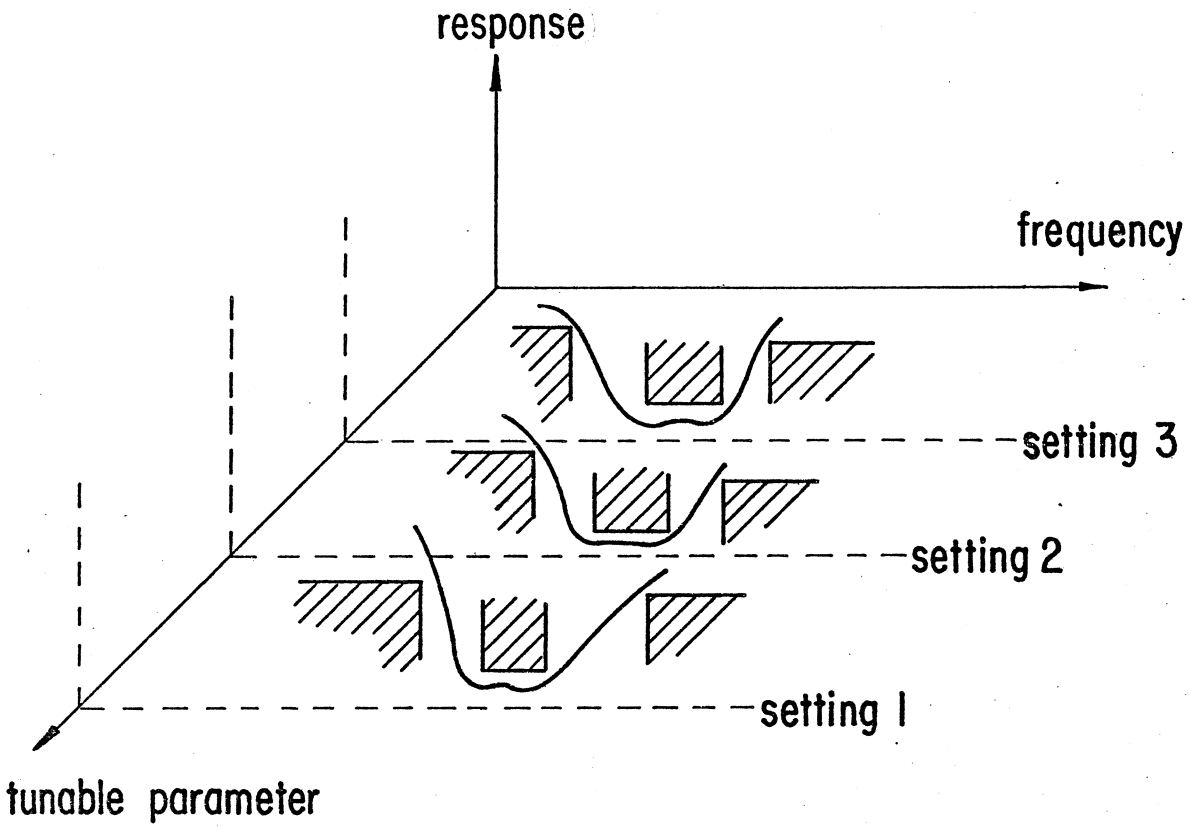
response
frequency
setting 3
setting 2
setting 1
tunable parameter

Fig. 1

(a)

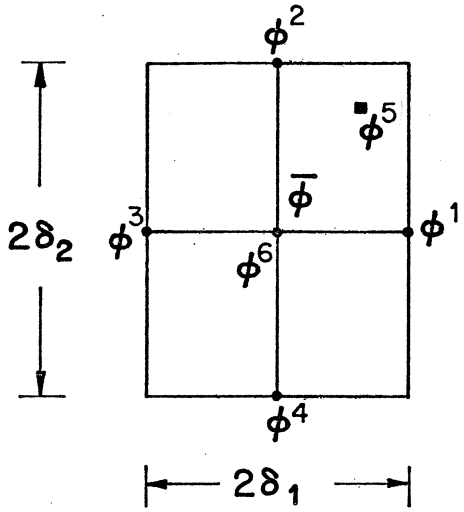
ϕ^2
ϕ^5
$\bar{\phi}$
$2\delta_2$
ϕ^3
ϕ^1
ϕ^6
ϕ^4
$2\delta_1$

(b)

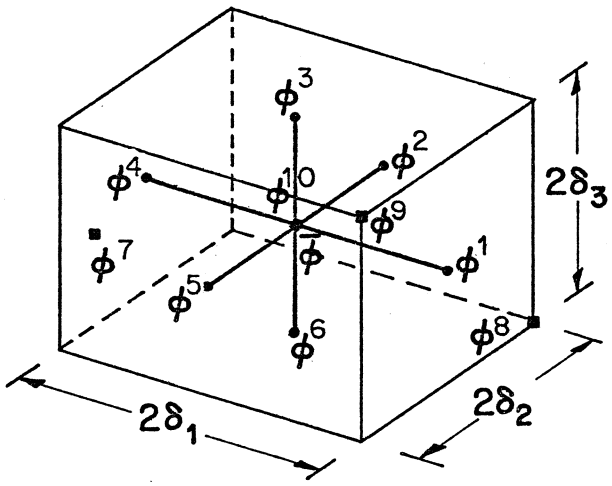
ϕ^3
ϕ^2
ϕ^4
ϕ^{10}
$2\delta_3$
ϕ^9
ϕ^7
$\bar{\phi}$
ϕ^1
ϕ^5
ϕ^6
ϕ^8
$2\delta_1$
$2\delta_2$

Fig. 3

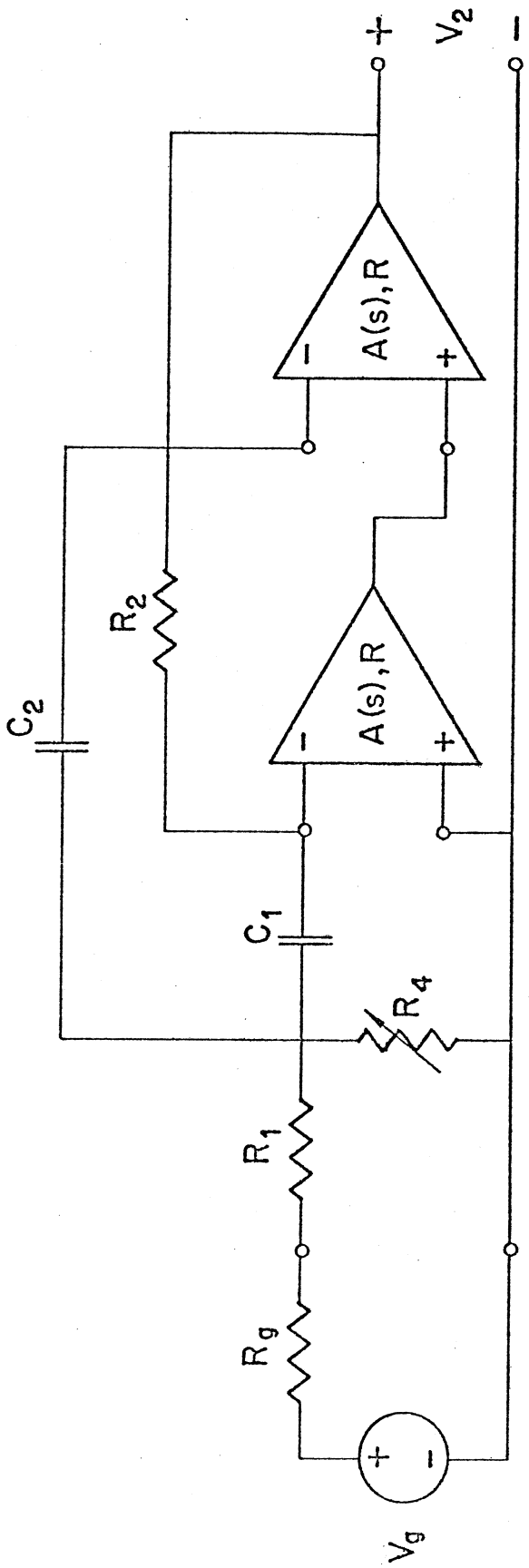

Fig. 5

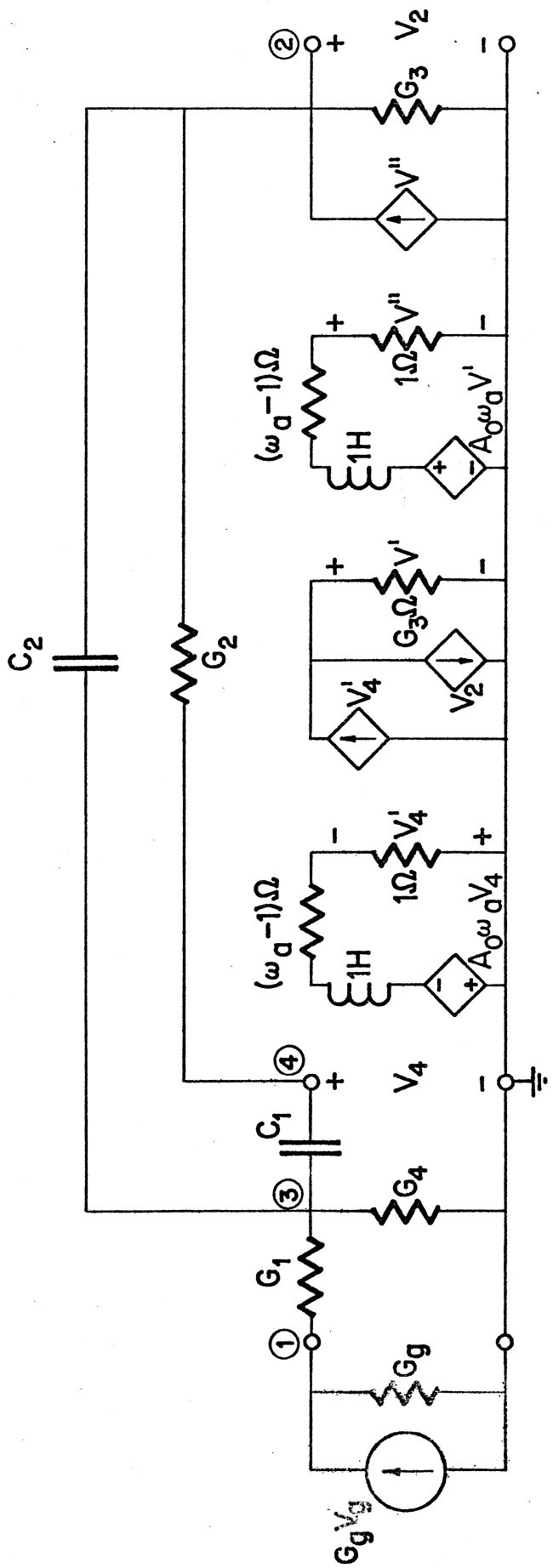
C2
G2
C1
G1
G4
G3
Gg
Gg Vg
V2
V4
V''
V'
V4'
1Ω
1H
(ωa−1)Ω
A0ωa V'
A0ωa V4
G3Ω
1
2
3
4

Fig. 7

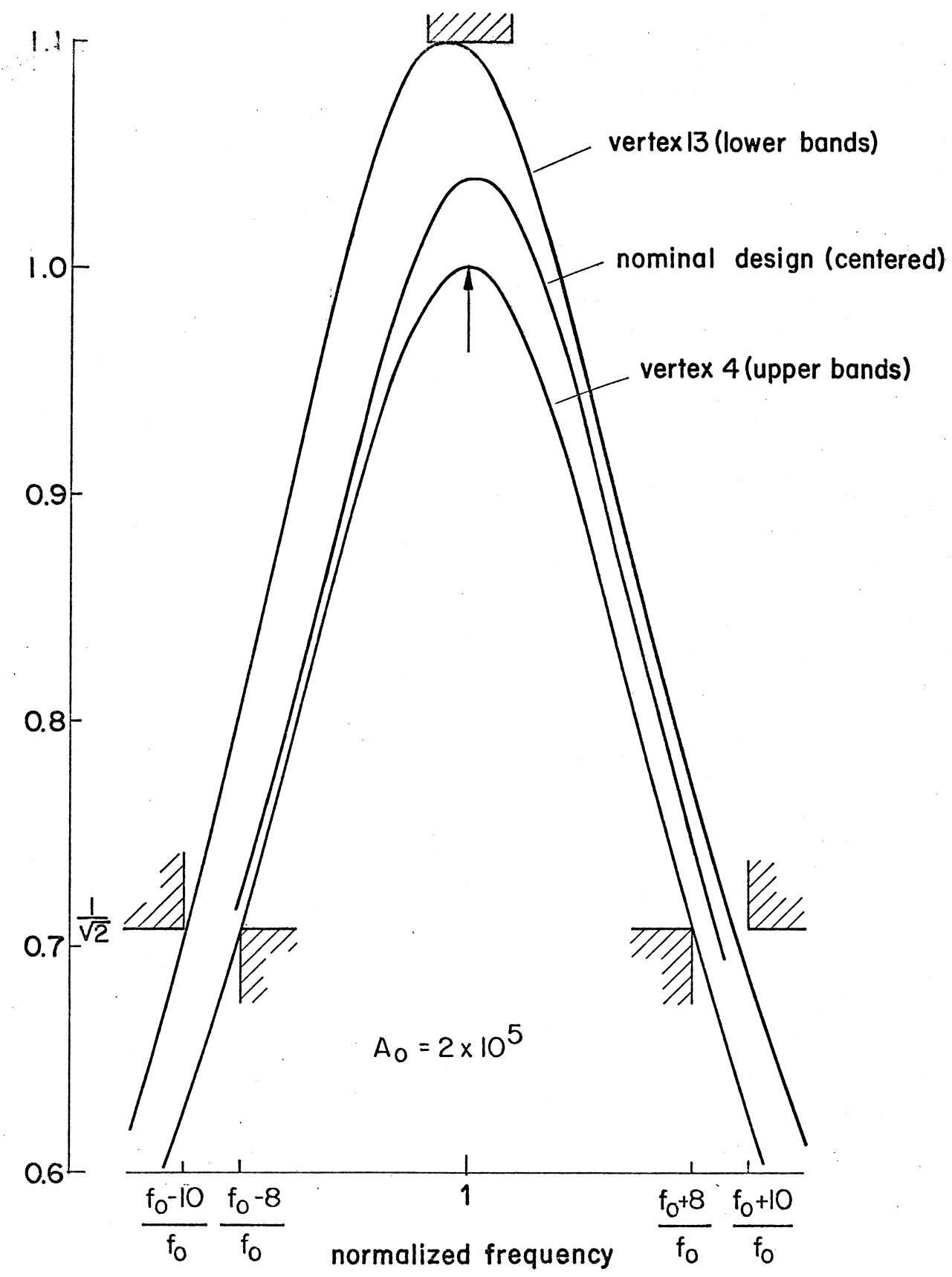
$|V_2|$
Design with 4 Tolerances, 3 Nominals
1.1
1.0
0.9
0.8
$\frac{1}{\sqrt{2}}$
0.7
0.6
vertex 13 (lower bands)
nominal design (centered)
vertex 4 (upper bands)
$A_0 = 2 \times 10^5$
$\frac{f_0-10}{f_0}$
$\frac{f_0-8}{f_0}$
1
$\frac{f_0+8}{f_0}$
$\frac{f_0+10}{f_0}$
normalized frequency

Fig. 9

(a)

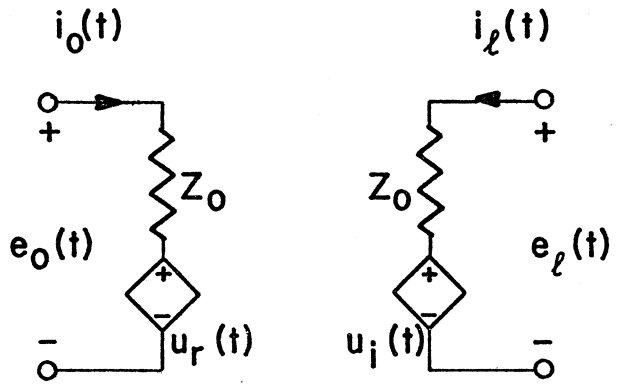

(b)

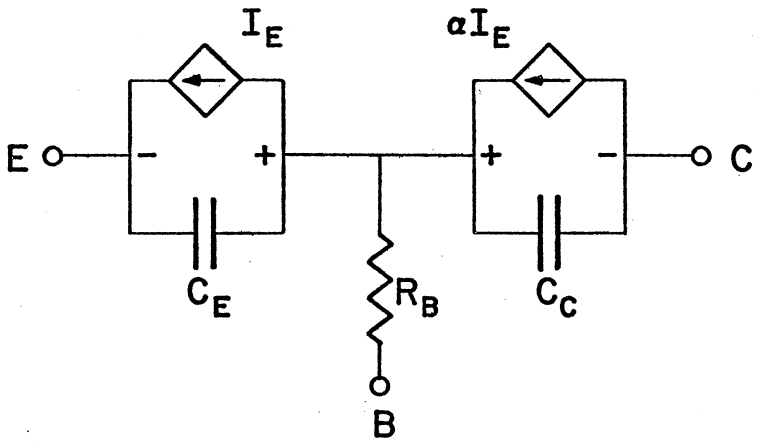

Fig. 11

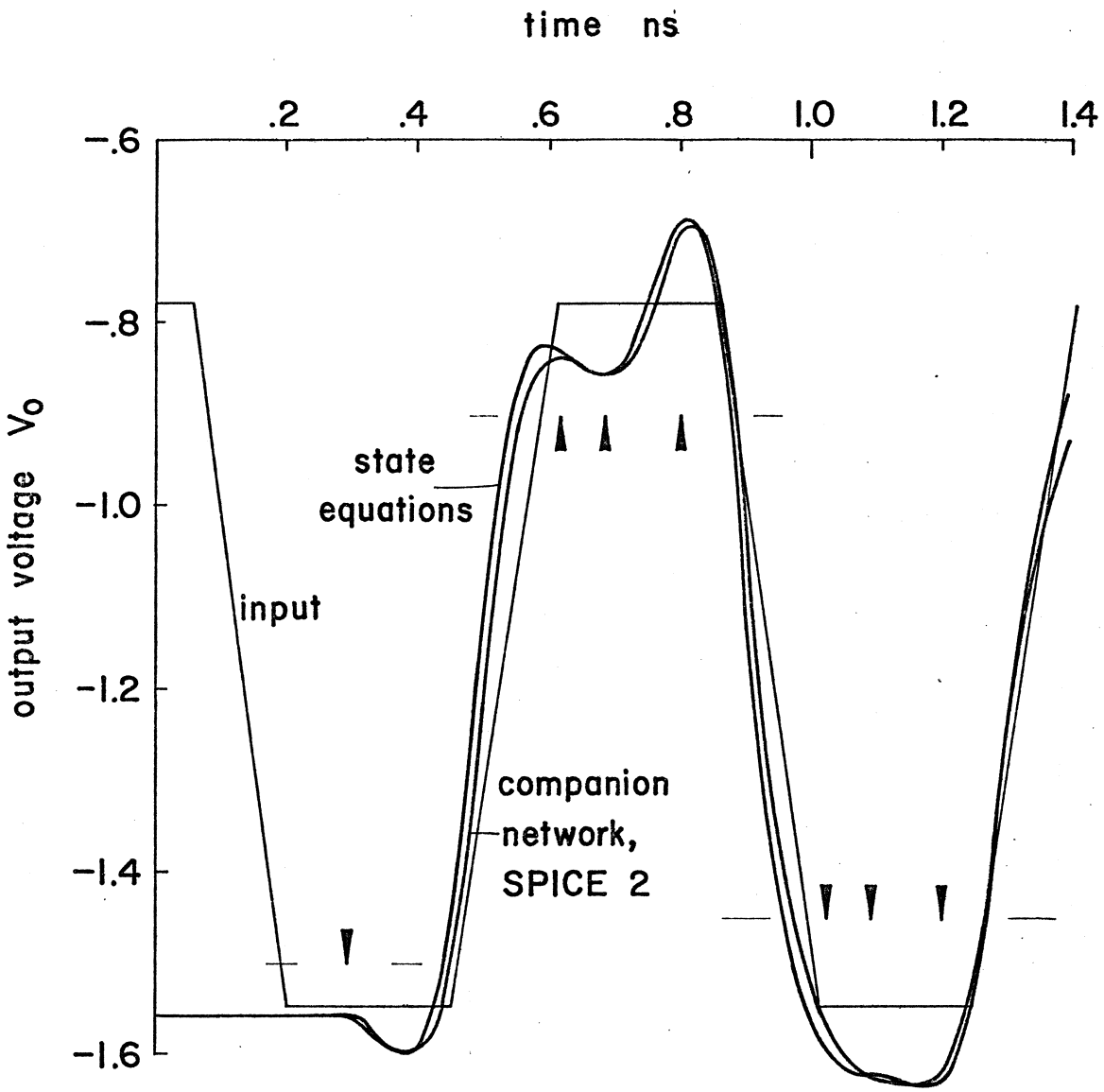
time ns
.2
.4
.6
.8
1.0
1.2
1.4
-.6
-.8
-1.0
-1.2
-1.4
-1.6
output voltage V_o
state
equations
input
companion
network,
SPICE 2

Fig. 13

I. INTRODUCTION

The trend in circuit analysis and optimization is increasingly towards consideration of production yield, design centering, optimal assignment of component tolerances and post-production tuning in an integrated fashion [1-4]. The scope and size of the resulting design problems have expanded immensely as a result. This paper explains how specially written or general circuit simulators such as SPICE2 [5] can be exploited to efficiently meet this goal without the explicit requirement of sensitivities.

The basic idea begins with using the designer's knowledge in establishing a nominal solution and associated tolerances and parameter distributions. One run of the simulator at $(k+1)(k+2)/2$ preselected sets of k parameter values leads to a set of quadratic models of the response w.r.t. the parameters. Those models are subsequently used to carry out the optimization processes, where the objective is (intuitively) to minimize production cost. The models may be updated and the process repeated depending upon the accuracy required and the conditioning of the problem. Available nonlinear programming packages are used to execute the worst-case designs, yield optimizations and designs with specified yield.

Detailed presentation of the mathematical background, and techniques for efficient selection and evaluation of candidates for worst case can be found in [2] and [6]. Explicit formulas for production yield and its sensitivities for arbitrary distributions [7] avoid iterative use of the Monte Carlo method.

The nonlinear optimization problem which can be formulated is directed at minimizing a cost function, usually involving one or more components of $\underset{\sim}{\phi}^0$, $\underset{\sim}{\varepsilon}$, $\underset{\sim}{t}_m$ and $\underset{\sim}{t}_c$ as variables while

$$\underset{\sim}{\phi} \in R_c(\underset{\sim}{\psi})$$

for all $\underset{\sim}{\mu}_\varepsilon$ and $\underset{\sim}{\psi}$ (independent variables associated with actual design specifications) and some corresponding $\underset{\sim}{\mu}_{tm}$ and $\underset{\sim}{\mu}_{tc}(\underset{\sim}{\psi})$. The family of constraint regions $R_c(\underset{\sim}{\psi})$ depends on model uncertainties and can be given in terms of inequality constraints by

$$R_c(\underset{\sim}{\psi}) \triangleq \{\underset{\sim}{\phi} \mid \underset{\sim}{g}(\underset{\sim}{\phi}, \underset{\sim}{\psi}) \geq \underset{\sim}{0} \text{ for all permissible } \underset{\sim}{\mu}_\delta\} \quad . \tag{2}$$

III. RESPONSE AND FUNCTION EVALUATION

The Quadratic Polynomial

Quadratic models of the circuit response w.r.t. the parameters at appropriate sample points in the frequency or time domains permit the use of general purpose simulators without explicit requirement of sensitivities. These models are subsequently used to carry out the optimization process. The models may be updated and the process repeated depending on the accuracy required and the conditioning of the problem.

To minimize computational effort, the simulator should provide responses at $(k+1)(k+2)/2$ base points, where k is the dimension of $\underset{\sim}{\phi}$, suitably arranged within an interpolation region described by

$$\bar{\underset{\sim}{\phi}} - \underset{\sim}{\delta} \leq \underset{\sim}{\phi} \leq \bar{\underset{\sim}{\phi}} + \underset{\sim}{\delta} \quad , \tag{3}$$

where $\bar{\underset{\sim}{\phi}}$ is the center of the interpolation region and $\underset{\sim}{\delta}$ defines the size. See Fig. 3 for the arrangement of the base points. Full details of theoretical aspects are given in [4].

where s is the complex frequency variable, $A_0 = 2 \times 10^5$ is the d.c. gain and $\omega_a = 12\pi$ rad/s the 3dB radian bandwidth. Furthermore, a nonzero output resistance R is assumed for the operational amplifier(s).

The second amplifier in the cascade is designed to stabilize the filter for higher frequencies. The ideal transfer function, i.e., for $A_0 \to \infty$ and $R \to 0$ is easily shown to be, using Fig. 6 and assuming $R_g = 0$

$$\frac{V_2}{V_g} = - G_1 \frac{sC_1}{s^2C_1C_2+sG_2(C_1+C_2)+G_2(G_4+G_1)} . \tag{5}$$

The maximum value of $F = |V_2/V_g|$, denoted by $\hat{F}$, occurs at

$$\omega_0 = \sqrt{G_2(G_1+G_4)/(C_1C_2)} \tag{6}$$

and is given by

$$\hat{F} = \frac{G_1C_1}{G_2(C_1+C_2)} . \tag{7}$$

The corresponding 3dB radian bandwidth Ω is given by

$$\Omega = \frac{G_2(C_1+C_2)}{C_1C_2} . \tag{8}$$

Expressions (5)-(8) indicate the basic behaviour of the filter from which it is seen that R_4 alone can be used for tuning without affecting $\hat{F}$ or Ω. One can nominally select $C_1 = C_2 = C$ and R_2 as fixed and optimize R_1 and C so that C determines the bandwidth and R_1 is subsequently adjusted to yield the desired $\hat{F}$. The expressions can also be used to simplify the selection of candidates for worst-case designs.

The nodal equations for the nonideal filter can be assembled in matrix form as

specification of 1.1 was taken at 98, 99, 100, 101 and 102 Hz, and $1/\sqrt{2}$ at 90 and 110 Hz. A lower specification of $1/\sqrt{2}$ was taken at 92 and 108 Hz, and 1 at 100 Hz. The objective function was

$$U = \frac{R_1^0}{\varepsilon_1} + 2\,\frac{C^0}{\varepsilon_2} \,. \tag{10}$$

Including 8 variables for R_4, one for each of eight vertices considered, the total number was 12. FLOPT4 [9] carried out the optimization in conjunction with the Bandler-Charalambous minimax approach to nonlinear programming [10].

Table I summarizes the results obtained starting at R_1^0 = 10 kΩ, C^0 = 0.75 μF, $\varepsilon_1/R_1^0 = \varepsilon_2/C^0$ = 3% and R_4 = 200 Ω. R_2 is fixed at 26.5 kΩ. Fig. 8 shows the responses for the active vertices, namely, $\underset{\sim}{\mu}^4 = [1\ 1\ -1]^T$ and $\underset{\sim}{\mu}^5 = [-1\ -1\ 1]^T$ (the variables are ordered as R_1, C_2, C_1). All running times are for a CDC 6400.

Also shown in Table I and Fig. 8 are (indistinguishable) results of using quadratic models obtained from SPICE2. Interpolation was conducted around the starting point for variables R_1, C_2, C_1 and R_4. In the first modeling problem of Table I the constraint region was represented by one interpolation region which has been updated once (this is the reason for the two runs of SPICE2). The tolerances on the elements tended to be greater than the size of the interpolation region $\underset{\sim}{\delta}$ which led to the interpolation around each of the 8 vertices. This interpolations was updated once leading to a total number of 4 runs for the second modeling problem.

Another problem considered is the optimal assignment of the relative tolerances ε_{R1}/R_1^0, ε_{C2}/C^0, ε_{C1}/C^0 and ε_{R2}/R_2^0 with R_4 as a customer tunable variable to meet the specifications with $100 \leq f_0 \leq 700$

for the characteristic impedance Z_0 and 0.25 ns for the delay time τ. Fig. 12 shows the input voltage E_1 and time point constraints used. The circuit is initially at equilibrium with E_1 = -0.776V. Required analyses were carried out via the state equations and Gear's integration scheme [13, 14]. Full details are available [15, 16]. Each constraint is described by a quadratic polynomial [17] having 15 coefficients and used in the minimization of

$$U = \frac{E_4^0}{\varepsilon_1} + \frac{Z_0^0}{\varepsilon_2} + \frac{R_4^0}{\varepsilon_3} + \frac{C_0^0}{\varepsilon_4} \quad , \tag{12}$$

to produce a worst-case design w.r.t. these 8 variables. The results are shown in Table IV and Fig. 12. Only 30 integrations were necessary (model updated once) at a cost of 48 s CPU time.

The analysis of the CSEF was also performed using SPICE2. In order to overcome the problem of handling a nonlinear capacitance in the form of the one given in the transistor model (Fig. 11(b)), the current passing through the nonlinear part of the capacitance was represented by the current i_1 of a two-dimensional current controlled current source. The currents controlling this source are i_2 and i_3 in two small additional networks as shown in Fig. 13. The coefficients of the polynomial representing i_1, are all zero except the coefficient of the cross term, which has the value one. In the circuit through which i_2 is passing $P_0 = P_1 I_S$ so as to let i_2 be equal to $P_1 I_S \exp(\theta V_{BE})$. The current I_S will represent dV_{BE}/dt. The results were checked by Rizk [18] using the companion network approach [19]. The running time was 40 s.

Fig. 12 also shows the response obtained using the built-in models in SPICE2. Here, the parameter values are set in such a way as to match as closely as possible the transistor model used in the state variable

[3] J.W. Bandler and H.L. Abdel-Malek, "Optimal centering, tolerancing and yield determination using multidimensional approximations", Proc. IEEE Int. Symp. Circuits and Systems (Phoenix, AZ, 1977), pp. 219-222.

[4] J.W. Bandler and H.L. Abdel-Malek, "Optimal centering, tolerancing and yield determination via updated approximations and cuts", Faculty of Engineering, McMaster University, Hamilton, Canada, Report SOC-173, 1977. To appear in IEEE Trans. Circuits and Systems.

[5] L.W. Nagel, "SPICE2: A program to simulate semiconductor circuits", Electronics Research Lab., Univ. of California, Berkeley, Memo. No. ERL-M520, 1975.

[6] J.W. Bandler, "Nonlinear optimization of engineering design with emphasis on centering, tolerancing and tuning", in Large Engineering Systems, A. Wexler, Ed. Oxford, England: Pergamon, 1977.

[7] H.L. Abdel-Malek and J.W. Bandler, "Yield estimation for efficient design centering assuming arbitrary statistical distrubtions", Int. J. Circuit Theory and Applications, vol. 6, 1978.

[8] A. Budak and E.R. Zeller, "Practical design considerations for a variable center frequency, constant bandwidth, and constant peak-value active filter", IEEE J. Solid-State Circuits, vol. SC-7, 1972, pp. 308-311.

[9] J.W. Bandler and D. Sinha, "FLOPT4 - a program for least pth optimization with extrapolation to minimax solutions", Faculty of Engineering, McMaster University, Hamilton, Canada, Report SOC-151, 1977.

[10] J.W. Bandler and C. Charalambous, "Nonlinear programming using minimax techniques", J. Optimization Theory and Applications, vol. 13, 1974, pp. 607-619.

[11] J.W. Bandler, J.H.K. Chen, P. Dalsgaard and P.C. Liu, "TOLOPT - a program for optimal, continuous or discrete, design centering and tolerancing", Faculty of Engineering, McMaster University, Hamilton, Canada, Report SOC-105, 1975.

[12] C.W. Ho, "Time-domain sensitivity computation for networks containing transmission lines", IEEE Trans. Circuit Theory, vol. CT-18, 1971, pp. 114-122.

[13] C.W. Gear, "The automatic integration of differential equations", Comm. ACM., vol. 14, 1971, pp. 176-179.

[14] Subroutine DVOGER: International Mathematical and Statistical Libraries, IMSL Library 3, Edition 5 (FORTRAN) CDC 6000/7000.

[15] H.L. Abdel-Malek, "A unified treatment of yield analysis, worst-

TABLE I RESULTS FOR FIXED SPECIFICATIONS

Method	R_1^0 (kΩ)	C^0 (μF)	ε_1/R_1^0 (%)	ε_2/C^0 (%)	R_4 (Ω)	CPU time (min)
SPICE2 (modeling)†	12.52	0.721	2.1	2.7	177-200	2
SPICE2 (modeling)††	12.57	0.722	2.0	2.9	177-200	4
special (exact)	12.57	0.723	2.0	2.9	178-200	1.7

† Only 2 (†† only 4) runs of SPICE2.

TABLE II RESULTS BY TOLOPT FOR TUNABLE SPECIFICATONS

R_1^0 (kΩ)	C^0 (μF)	R_2^0 (kΩ)	ε_{R1}/R_1^0 (%)	ε_{C1}/C^0 (%)	ε_{C2}/C^0 (%)	ε_{R2}/R^0 (%)	R_4 (Ω)
14.0	6.5	30.0	1.2	1.7	1.6	1.2	3.7-216

TABLE III(c)

TRANSISTOR MODEL PARAMETERS

I_S	saturation current	0.6×10^{-9} A
α	common base current gain	0.99
R_B	base resistance	50.0 Ω
C_C	collector junction capacitance	0.5 pF
C_{JE}	emitter junction depletion layer capacitance	0.12 pF
TT	base transit time	0.01 ns
θ	inverse of thermal potential	$38.668\ V^{-1}$

$$I_E = I_S\,(\exp(\theta V_{BE})-1)$$

$$I_C = \alpha\, I_E$$

$$C_E = C_{JE} + TT\,\frac{dI_E}{dV_{BE}}$$

R_B and C_C are assumed zero for transistor T_3

TABLE IV WORST-CASE DESIGN OF THE CSEF

E_4^0 (V)	Z_0^0 (Ω)	R_4^0 (Ω)	C_0^0 (pF)	ε_1/E_4^0 (%)	ε_2/Z_0^0 (%)	ε_3/R_4^0 (%)	ε_4/C_0^0 (%)	CPU time (min)
1.66	92	45.5	1.25	4.5	8.3	13.8	14.0	1.7

Only 30 integrations (48 s, CPU time) necessary (model updated once).

Fig. 10 Current switch emitter follower (CSEF) circuit.

Fig. 11 Equivalent circuits of (a) the lossless transmission line,

$$u_i(t) = [e_0(t-\tau) + Z_0\, i_0(t-\tau)]\, U(t-\tau) + \Phi_i(t),$$

$$u_r(t) = [e_\ell(t-\tau) + Z_0\, i_\ell(t-\tau)]\, U(t-\tau) + \Phi_r(t),$$

where Φ represents the initial voltage distribution on the line and U is the step function given by

$$U(t-\tau) = \begin{cases} 0 & t < \tau\ , \\ 1 & t \geq \tau\ , \end{cases}$$

(b) the transistor model.

Fig. 12 Input voltage, specifications at specific time points and worst-case nominal responses.

Fig. 13 Transistor model described to SPICE2.

Fig. 14 Nominal responses after yield optimization.

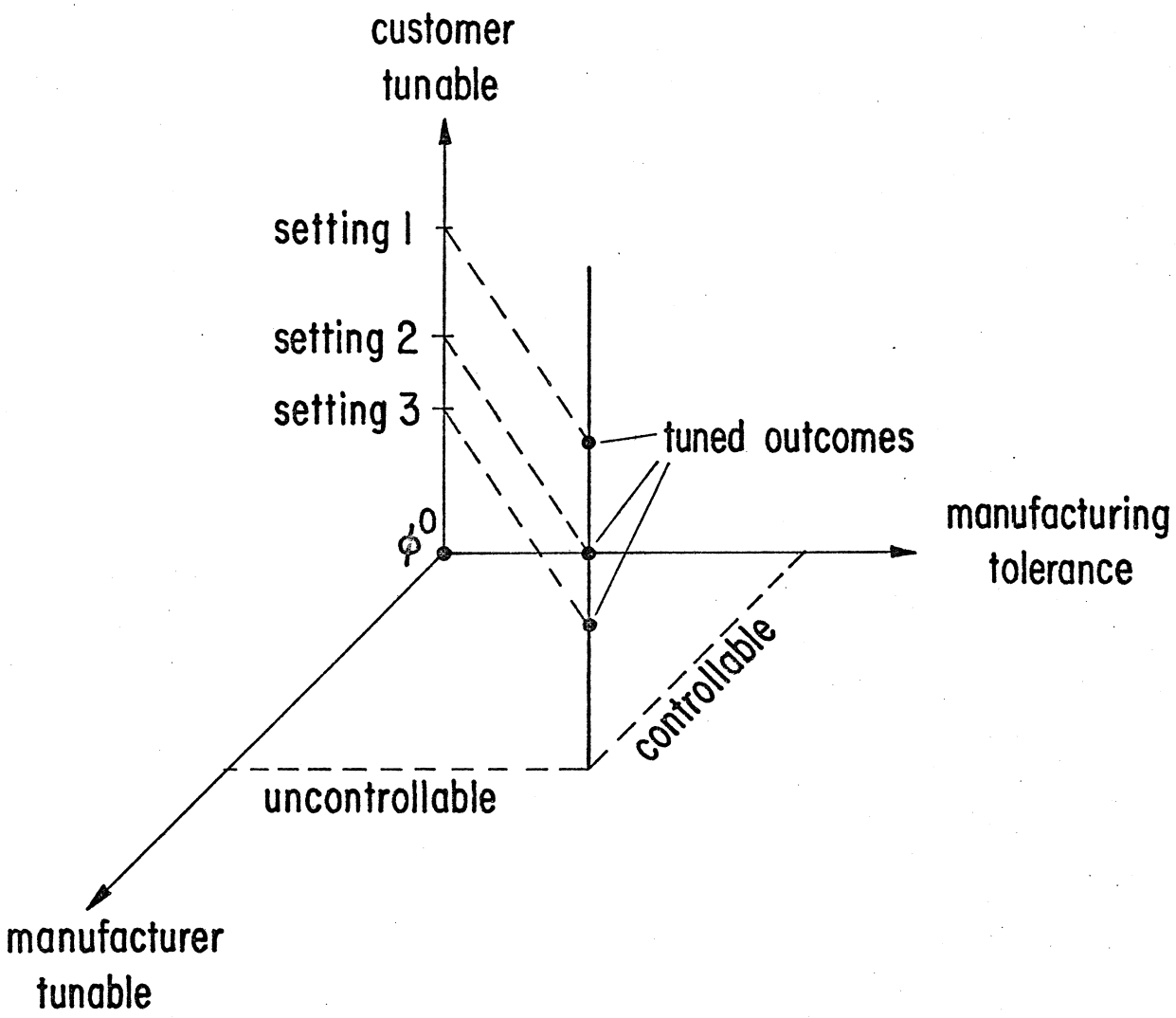
customer
tunable
setting 1
setting 2
setting 3
tuned outcomes
φ^0
manufacturing
tolerance
controllable
uncontrollable
manufacturer
tunable

Fig. 2

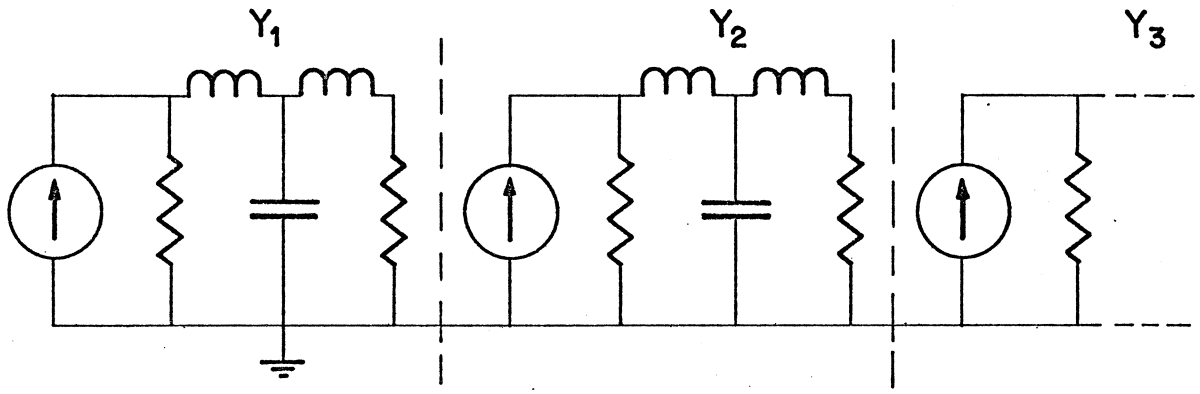

Fig. 4

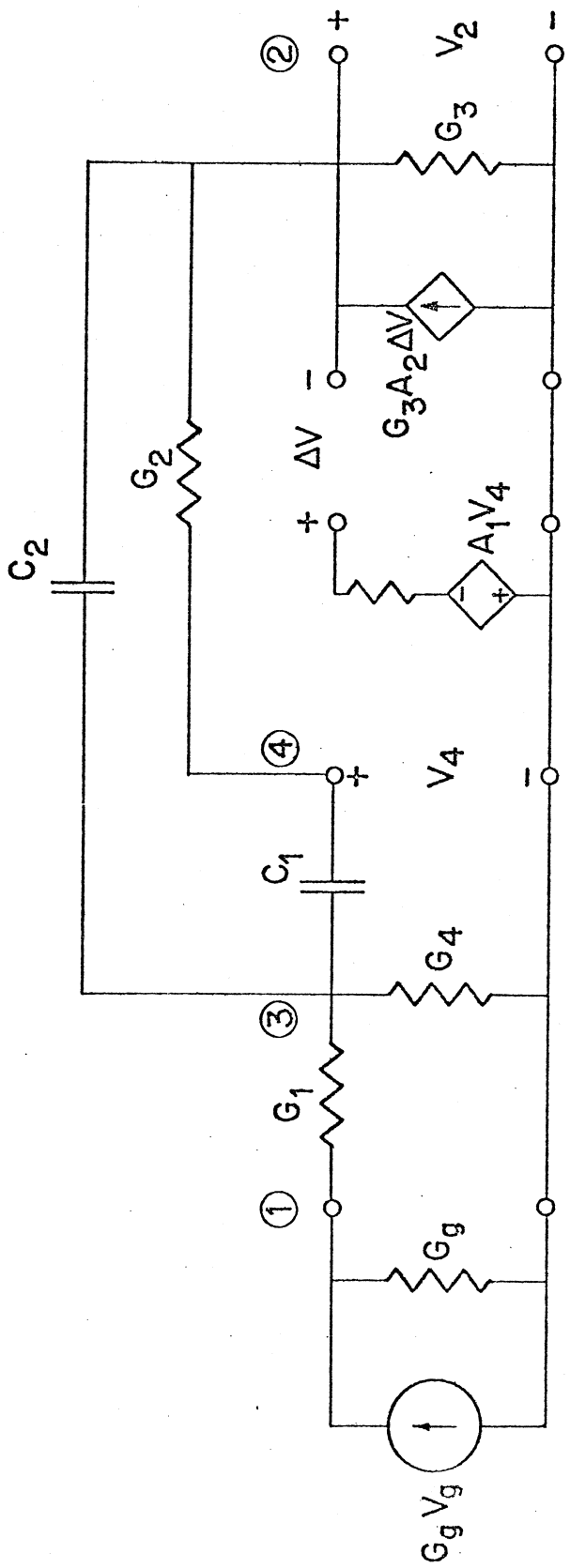

Fig. 6

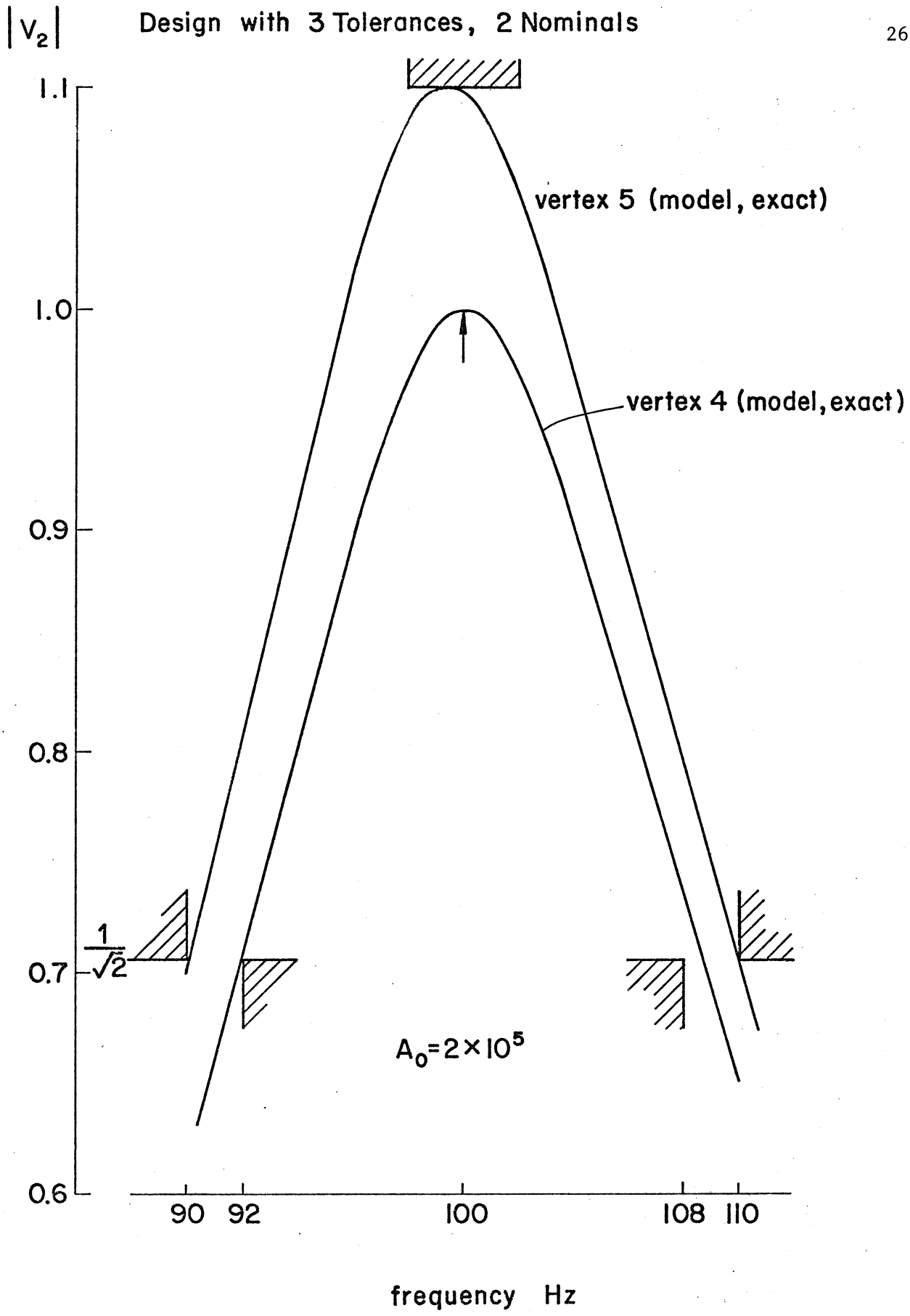
|V2|
Design with 3 Tolerances, 2 Nominals
1.1
1.0
0.9
0.8
0.7
0.6
1/√2
vertex 5 (model, exact)
vertex 4 (model, exact)
A0=2×10^5
90
92
100
108
110
frequency Hz

Fig. 8

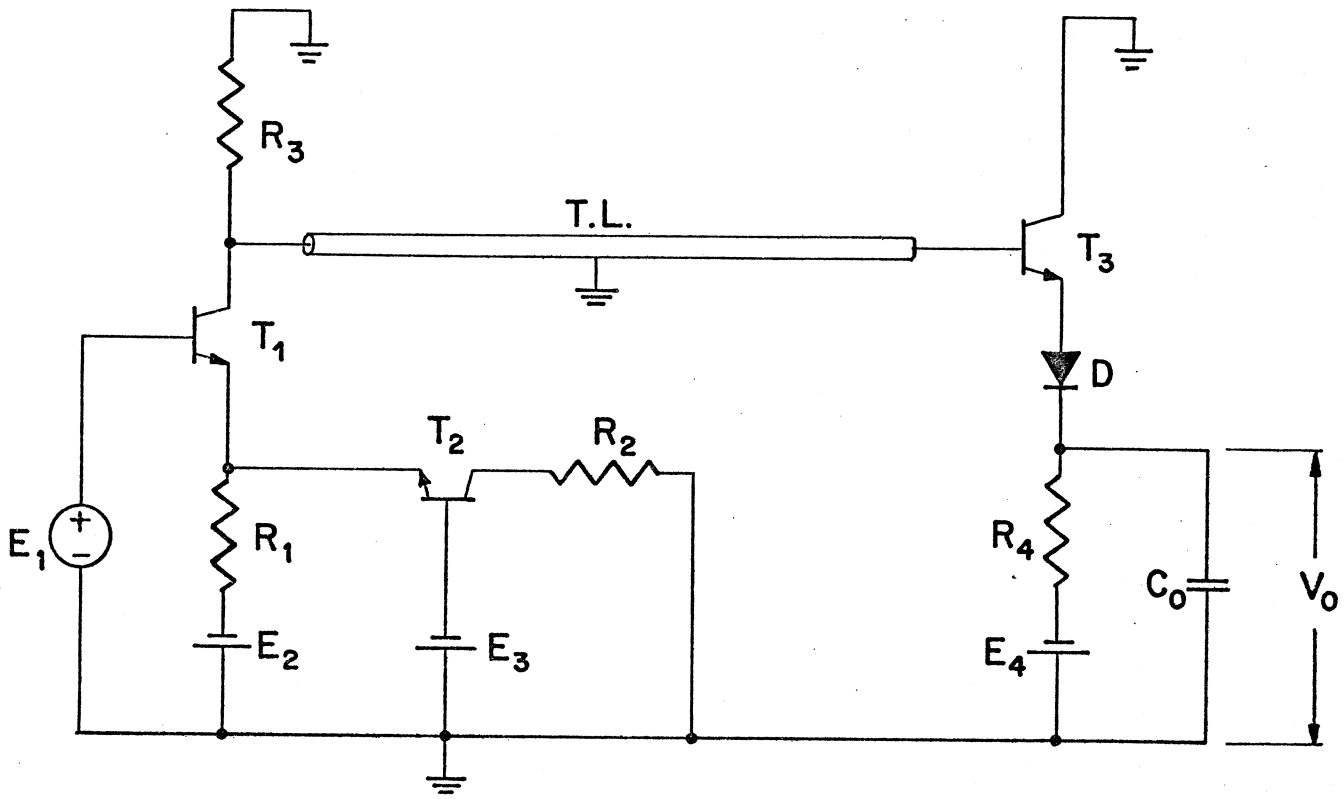

Fig. 10

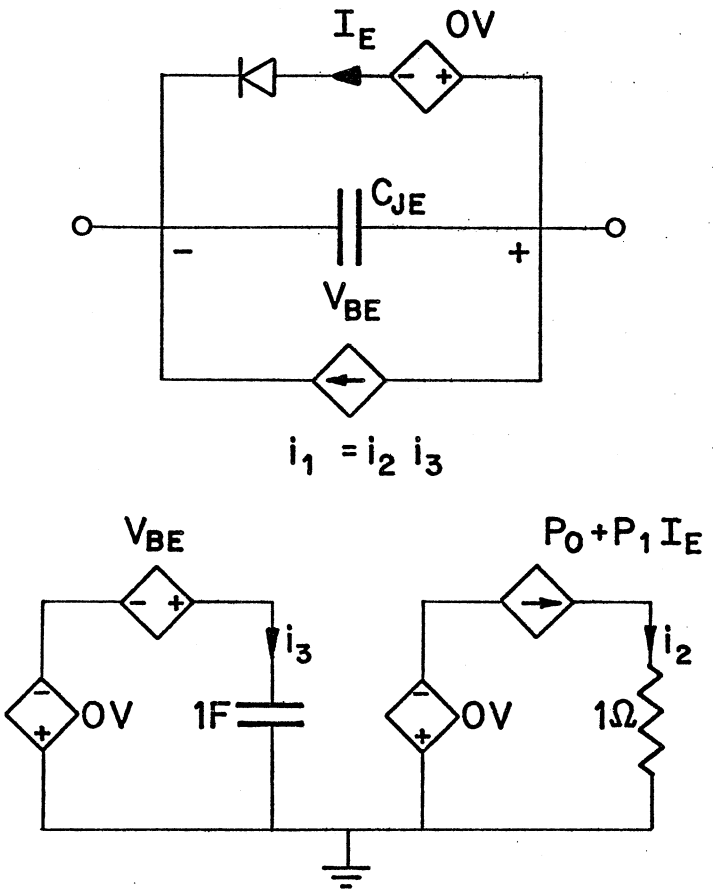

Fig. 12

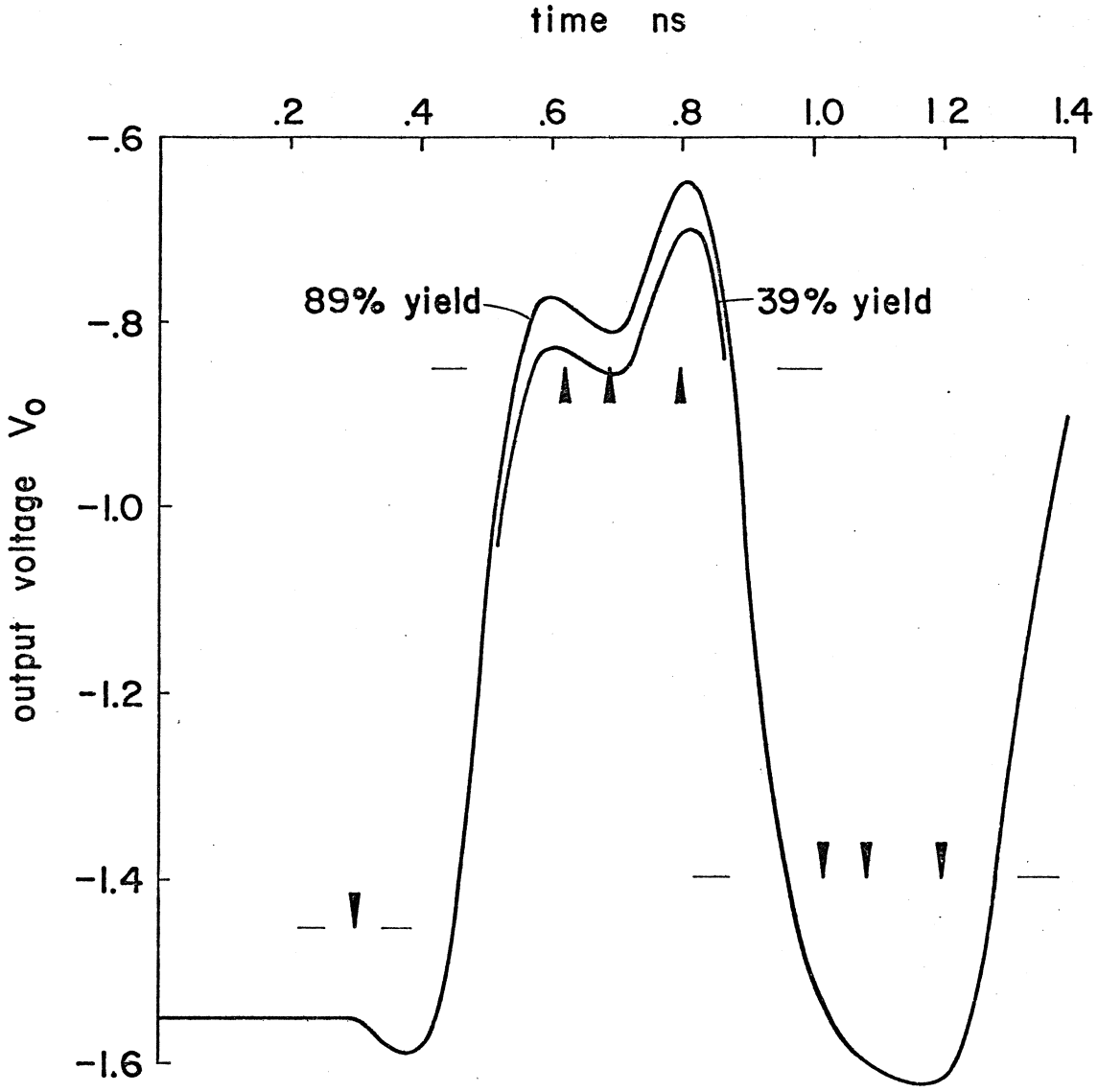
time ns
.2
.4
.6
.8
1.0
1.2
1.4
-.6
-.8
-1.0
-1.2
-1.4
-1.6
output voltage V_o
89% yield
39% yield

Fig. 14